Synthesis and fluorescence properties of reddish-orange emitting (Y, Ga)PO$_4$: Sm^{3+} powder phosphors

U. RAMBABU[a], SANG-DO HAN[a*], S. SAILAJA[b], B. SUDHAKAR REDDY[b]
[a] *Korea Institute of Energy Research (KIER), Daejeon, 305-343, Republic of Korea*
[b] *Department of Physics (Research Centre), S.V. Degree College, Kadapa - 516003, India*

(Y$_{1-x-y}$, Ga$_x$)PO$_4$: Sm$_y^{3+}$ (where $0.2375 \leq x \leq 0.95$; $y = 0.05$ moles), powder phosphors have been synthesized through a novel co-precipitation technique, followed by calcination. The produced phosphors have been characterized by various spectroscopic techniques. From the XRD patterns, it is confirmed that the produced phosphors possess good crystalinity with tetragonal phase. The evidence for phosphate functional groups was investigated by Fourier transform - Infrared (FT-IR) spectra. Scanning electron microscopy (SEM) measurement reveals that the crystallite shape and size of the phosphors have been prominently dominated by the host composition (Y, Ga)PO$_4$. YPO$_4$: Sm^{3+} phosphor has shown spindle like shape crystallites, (Y, Ga)PO$_4$: Sm^{3+} phosphors are in a gel type leafy shape and GaPO$_4$: Sm^{3+} has shown agglomerated particles of spherical shape with an average crystallite size, at around 100 nm. These phosphors have exhibited strong reddish (^{4}G$_{5/2} \rightarrow$ ^{6}H$_{9/2}$) – orange (^{4}G$_{5/2} \rightarrow$ ^{6}H$_{7/2}$) color, upon UV- excitation. From the fluorescence spectra, it is obvious that the gallium content has strongly influenced the fluorescence behavior of these phosphors. On the basis of fluorescence and pertinent optical properties the phosphor with composition Y$_{0.95}$PO$_4$: Sm$_{0.05}^{3+}$ has suggested to be an appropriate luminescent material for their use in certain optical display devices for reddish-orange emission.

1. Introduction

Rare earth activated phosphors have attracted a great deal of interest because of their marked improvements in lumen output, color rendering index, energy efficiency, and eminent radiation stability [1-4]. Recently, many efforts have been paid to the white light emitting diodes (WLEDs) because of their advantages such as high efficiency, more brightness, good reliability, low power consumption, free of toxic mercury, long lifetime, fast response, energy saving and environment friendliness. WLEDs are efficient lighting devices because of their small stokes shift. Based on these merits WLEDs are used for the replacement of incandescent/fluorescent lamps, solid state lighting sources and flash lights [5]. One of the easy methods to fabricate WLEDs is the combination of UV-LED with cyan - and orange-emitting phosphors [6-9]. Therefore, there is a great demand to search for a novel and superior orange light emitting phosphor material for WLEDs.

It is well known that, the host materials for phosphors are generally based on borates, phosphates, aluminates, silicates, tungstate, molybdates, vanadates, etc. Among them phosphates, also known as the multifunctional materials are the best host candidates for the preparation of luminescent materials. Because of their easy, low temperature synthesis, low cost and also having the excellent properties such as high thermal stability, high luminous efficiency [10]. Phosphate based phosphors are having wide applications in lighting and displays. On the other hand, Y$_2$O$_3$ is an excellent host material in rare earth ions and has the advantages such as high chemical stability, low volatility in vacuum; thus it has been widely used in field emission displays (FEDs), cathode ray tubes (CRTs) and thin film electroluminescence (TFEL) devices. Sm^{3+} is a prominent activator ion among the rare earths for producing intense orange light in various inorganic host lattices [11]. ZnGa$_2$O$_4$ is one of the most promising luminescent oxide materials which have attracted a wide attention for the blue emission [12-13]. Minami et al. have reported the high luminance multi-colour emissions from TFEL devices using a newly developed multicomponent oxide [(Y$_2$O$_3$)$_{1-x}$, (Ga$_2$O$_3$)$_x$]:Mn phosphors. They have reported that as the gallium content increases, the emission peaks did shift from yellow to green region [14].

In view of the above literature survey, we have chosen an inorganic host lattice as YPO$_4$ compound and the dopant ions as Sm^{3+}, where we would like to see the substitution effect of gallium on yttrium oxide, in terms of fluorescence properties. In the present investigation, we have reported a novel and commercially viable synthesis route for (Y, Ga) PO$_4$: Sm^{3+} powder phosphors, studied the effect of gallium content on fluorescence spectra and on the pertinent optical properties.

2. Experimental

2.1 Synthesis of $(Y_{1-x-y}, Ga_x) PO_4: Sm_y^{3+}$ (where $0.2375 \leq x \leq 0.95$; $y = 0.05$ moles) powder Phosphors

Generally, phosphors were prepared by a conventional solid state reaction technique at elevated temperatures. Although, simply operated this method has several disadvantages including high temperature processing, long calcination time, repeated milling/grinding, inhomogeneity and the presence of different phases in the final product. Several solution based synthesis techniques, such as Sol-Gel [12], co- precipitation [13], spray pyrolysis, hydrothermal and solvothermal methods have been developed to counter the disadvantages of conventional solid state reaction technique [15,16]. For the synthesis of the proposed Sm^{3+}- activated phosphate phosphors, a co-precipitation technique followed by calcination was adopted, where the starting precursors were supposed to react at micro level and leads to homogeneous better product. Based on our previous reports on phosphate phosphors [17, 18], the concentration of the dopant, Sm^{3+}-ion has been fixed as 0.05 moles.

Firstly, Y_2O_3, Ga_2O_3 and Sm_2O_3 of purity 99.99% of Aldrich make with their stoichiometric ratios were initially dissolved in aqueous hydrochloric acid with moderate heating. The resultant solutions were stirred with the addition of ethylene glycol on a hot plate cum stirrer for uniform mixing for an hour, where the solvent ethylene glycol was used as a surfactant media. The obtained solution was precipitated with a certain volume of aqueous phosphoric acid, with drop wise addition under constant stirring. The pH of the reaction was maintained at around 6.5 to 7 with ammonium hydroxide (NH_4OH), where a dense white precipitation was formed. This precipitate was centrifuged and filtered, which was washed thoroughly with DI water and ethanol to remove the unreacted remnants, moreover the traces of ethylene glycol. The filtrate was dried in an electric oven at 120 ^{o}C. The dried powders were further heat treated at 900 ^{o}C for an hour. Thus, the produced phosphors were crushed into fine powder and stored in a polyethylene (PE) container for further characterization. The above methodology was adopted for the synthesis of all the reported phosphors as per their stoichiometric ratios.

2.2 Characterization

The phase purity of the synthesized powder phosphors were studied by Rigaku X-ray diffractometer with CuK_α radiation ($\lambda = 1.5406$ A^o) at 30 KV, tube voltage and 15 mA, current, where the diffraction angle 2θ was in the range, $10 \leq 2\theta \leq 80^o$ with a scanning rate of 1.2^o min^{-1}. The SEM images were measured using Hitachi S-3700N Scanning Electron Microscope (SEM). The instrumental parameters like accelerating voltage, working distance and magnification scale bar were mentioned on each SEM micrograph. The FT-IR spectra, in the range 4000-450 cm^{-1} were recorded on a Brucker Tensor 27,

Spectrophotometer via potassium bromide (KBr) pellet technique. Both the excitation (380-450 nm) and emission spectra (500-750 nm) were recorded on a SPEX Fluorolog - 2, Spectofluorometer (Model II) with data max software to acquire the data with a Xe - Arc lamp (150 W) as an excitation source.

3. Results and discussion

The phase purity of the phosphors synthesized was checked with X- ray diffractometer (XRD).The X-ray diffraction profiles of (a) $Y_{0.95}PO_4$: Sm^{3+}, (b) $(Y_{0.475}, Ga_{0.475}) PO_4$: Sm^{3+} and (c) $Ga_{0.95}PO_4$: Sm^{3+} powder phosphors have been shown in Fig. 1. XRD patterns revealed that the powders heat treated at 900 ^{o}C were well crystallized. The major diffraction peak positions of the XRD patterns are found to be consistent with the tetragonal xenotime structure, known from the bulk yttrium vanadate material (space group: 141 / amd). The diffraction peaks are in good agreement with the standard JCPDS, card no: 09-377. From the XRD profiles it is obvious that the diffraction peak intensities of $Ga_{0.95}PO_4$- Sm^{3+} phosphor are more intense than the YPO_4 and (Y, Ga) PO_4 hosted phosphors.
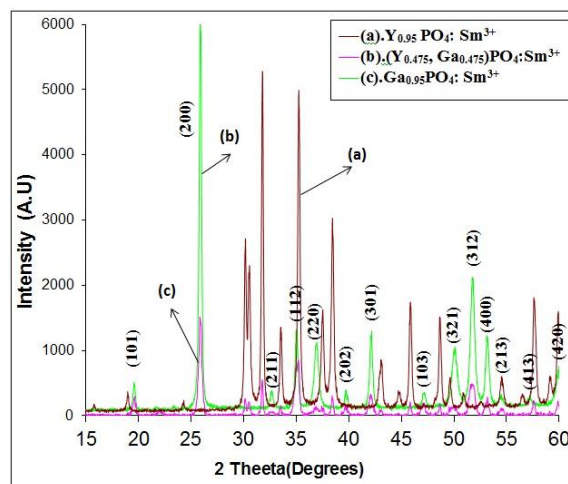

Fig. 1.   X-ray diffraction profiles of (a) $Y_{0.95}PO_4$: Sm^{3+}, (b) $(Y_{0.475}, Ga_{0.475}) PO_4$: Sm^{3+} and   (c) $Ga_{0.95}PO_4$: Sm^{3+}, powder phosphors.

The surface morphology and crystallite size of the produced powder phosphors were measured with a scanning electron microscope (SEM). Fig. 2 (a - c) shows the SEM images of (a) $Y_{0.95}PO_4$: Sm^{3+}, (b) $(Y_{0.475}, Ga_{0.475}) PO_4$: Sm^{3+} and (c) $Ga_{0.95} PO_4$: Sm^{3+} powder phosphors, respectively. SEM measurements reveals that the crystallite shape and sizes are prominently dominated by the host composition (Y, Ga), where $Y_{0.95}PO_4$: Sm^{3+} phosphor has shown spindle like shape crystallites, $(Y_{0.475}, Ga_{0.475}) PO_4$: Sm^{3+} phosphors are in a gel type leafy shape and $Ga_{0.95}PO_4$: Sm^{3+} has shown agglomerated spherical shape with an average particle size, at around 100 nm.
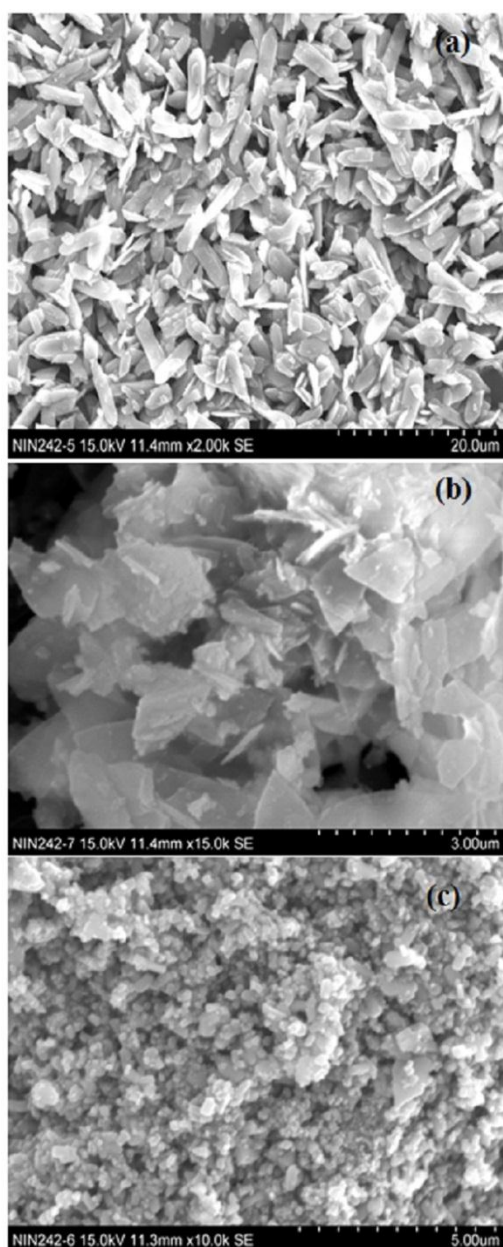
*Fig. 2. SEM images of (a) $Y_{0.95}PO_4$: Sm^{3+}, (b) $(Y_{0.475}, Ga_{0.475})$
PO_4: Sm^{3+} and (c) $Ga_{0.95}PO_4$: Sm^{3+}, powder phosphors.*

*Fig. 3. FTIR spectra of (a) $Y_{0.95}PO_4$: Sm^{3+}, (b) $(Y_{0.475}, Ga_{0.475})$
PO_4: Sm^{3+} and (c) $Ga_{0.95}PO_4$: Sm^{3+}, Powder phosphors.*

From the FT-IR spectra (Fig. 3), it was noted that for both the phosphors, $Y_{0.95}PO_4$: Sm^{3+} and $(Y_{0.475}, Ga_{0.475})$ PO_4: Sm^{3+}, the absorption peaks were noted to be similar. The bending vibrations of H_2O molecules and O-H stretching vibrations are present at about 1643 cm⁻¹ and in the range from 3430 to 2000 cm⁻¹, respectively [19]. Generally, the IR absorption bands of $(PO_4)^{3-}$ functional groups will be observed in two regions 1120-940 cm⁻¹ and 650-520 cm⁻¹, which are originated from O - P - O asymmetric bending vibration. In the present investigation, $(PO_4)^{3-}$ ions are characterized by the three IR absorption bands at 1048 cm⁻¹, 637 cm⁻¹ and 524 cm⁻¹, which are in well agreement with the reported literature [20-22].
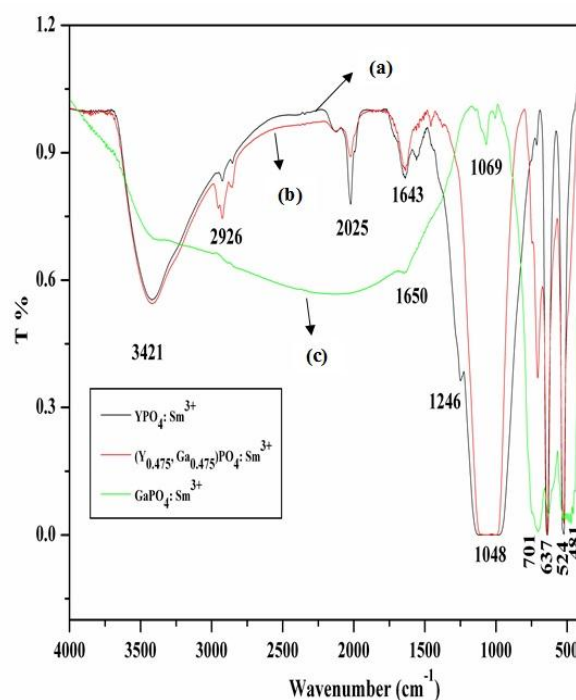
The excitation spectrum of Sm^{3+}- doped phosphor (Fig. 4) monitored with the emission wavelength at 601 nm, consists of several bands centered at 390 nm ($^6H_{5/2} \rightarrow$ $^6G_{11//2}$), 402 nm ($^6H_{5/2} \rightarrow$ $^4F_{7//2}$), 417 nm [$^6H_{5/2} \rightarrow$ $(^6P,^4P)_{11//2}$] and 439 nm ($^6H_{5/2} \rightarrow$ $^6G_{9//2}$) , which are the characteristic f - f transitions of the rare earth, Sm^{3+} - ions. The observed strongest peak at 402 nm, attributed to the $^6H_{5/2} \rightarrow$ $^4F_{7/2}$ transition, was fixed as an excitation wavelength in recording the emission spectra of all the phosphors. There was no obvious charge - transfer absorption of Sm^{3+}- O^{2-} interaction or host absorption band as usual [23]. This is because of Sm^{3+} ions interaction with the host lattice is very weak and no energy transfer occurs between Sm^{3+} ions and the host [24]. Upon the excitation at 402 nm, the emission spectra of Sm^{3+} - doped phosphors (Fig. 5) consists of the characteristic emission lines of Sm^{3+}, i.e.: $^4G_{5/2} \rightarrow$ $^6H_{5/2}$, $^4G_{5/2} \rightarrow$ $^6H_{7/2}$, $^4G_{5/2} \rightarrow$ $^6H_{9/2}$ and $^4G_{5/2} \rightarrow$ $^6H_{11/2}$ with the strongest peak at 601 nm, which emits reddish-orange light [24-26]. The first emission band at 563 nm, corresponding to the transition $^4G_{5/2} \rightarrow$ $^6H_{5/2}$ is a magnetic dipole, allowed one and is hard to the crystal field environment. The most prominent band located at 601 nm ($^4G_{5/2} \rightarrow$ $^6H_{7/2}$) is a magnetic dipole allowed transition and follows the selection rule $\Delta J = \pm 1$, but it is an electric dipole dominated one. Hence, it is a partially magnetic dipole allowed and partly a forced electric-dipole natured transition. The third band located at 644 nm is an electric dipole transition and is sensitive to the variations in the crystal field. Further, the intensity ratio of electric dipole to magnetic dipole transition will be used to know

the symmetry nature of the local environment around rare earth ions. In the present investigation, the electric dipole transition $^4G_{5/2} \rightarrow {^6H_{9/2}}$ at 644 nm is having the higher intensity than the magnetic dipole transition $^4G_{5/2} \rightarrow {^6H_{5/2}}$ located at 563 nm indicating the more asymmetric local environment around rare earth ions [27].
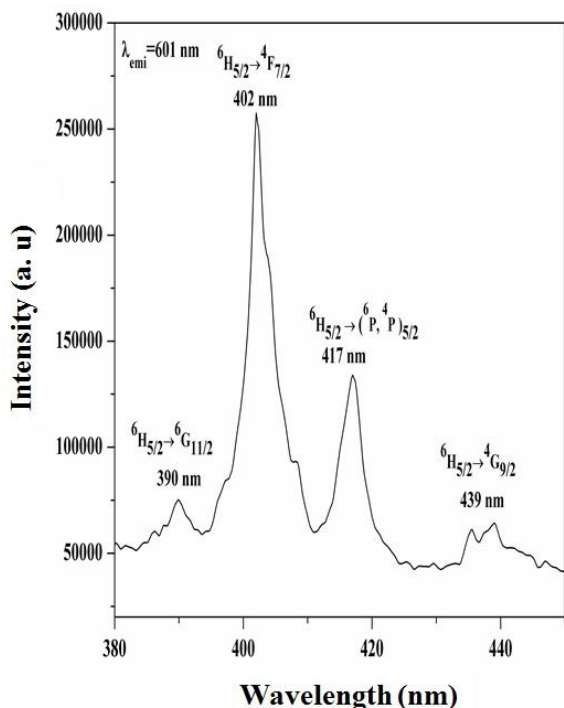

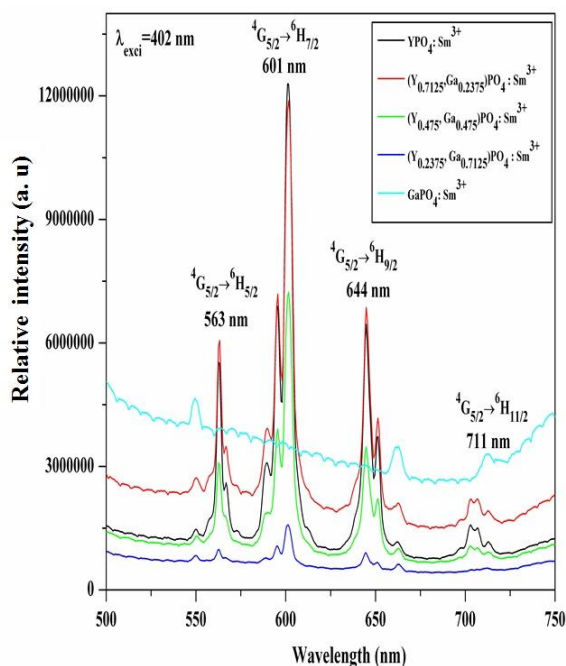*Fig. 4. Excitation spectrum of $Y_{0.95}PO_4$: Sm^{3+}, powder phosphor.*

Fig. 5. Fluorescence spectra of (a) $Y_{0.95}PO_4$: Sm^{3+}, (b) ($Y_{0.7125}$, $Ga_{0.2375}$) PO_4: Sm^{3+}, (c) ($Y_{0.475}$, $Ga_{0.475}$) PO_4: Sm^{3+}, (d) ($Y_{0.2375}$, $Ga_{0.7125}$) PO_4: Sm^{3+} and (e) $Ga_{0.95}PO_4$: Sm^{3+}, powder phosphors.

The emission magnitude of many phosphors tends to degrade gradually by several mechanisms. The activator ions can undergo change of valence (usually by oxidation), the crystal lattice degradation, atoms often the activators diffuse through the material, the surface undergoes chemical reactions with the environment with consequent loss of efficiency or build-up of an absorbing either the exciting or the radiated energy, etc. The fluorescence spectra elucidate the fluorescence intensity degradation with the increment of gallium content. Based on the ionic radii (ionic radii of Ga^{3+} is 0.62 Å, Y^{3+}- 0.9 Å and Sm^{3+}- 0.964 Å), Sm^{3+} ions have substituted Y^{3+}, rather than Ga^{3+} ions, where its ionic radii was relatively very small. Fluorescence quenching due to gallium substitution, can be explained as follows: when Ga^{3+} is in low concentration, the interaction between Ga^{3+}- Ga^{3+} was very limited. As the concentration increases, the Ga^{3+} ions are packed closer, which favored the transfer of excitation energy from one gallium ion to the next by resonance process, the energy eventually reached a sink (traps) from which it was dissipated via non-radiative process rather than the emission of light. However, the incorporation of gallium has distorted the crystal field surroundings of the activator, as a result affected the fluorescence behavior [28, 29].

4. Conclusions

In summary, it is concluded that $(Y_{(1-x-y)}, Ga_x) PO_4$: Sm_y^{3+} (where $0.2375 \leq x \leq 0.95$; y = 0.05 moles) powder phosphors have been successfully synthesized by a novel co-precipitation technique. XRD patterns, indicates that the produced phosphors are well crystalline and have the tetragonal phase. The phosphate functional groups of the obtained phosphors were confirmed by FT-IR, spectra. SEM measurements reveals that the crystallite shape and size of the phosphors are prominently dominated by the host composition (Y, Ga) PO_4, where YPO_4: Sm^{3+} phosphor has shown spindle like shape crystallites, dual (Y, Ga) PO_4: Sm^{3+} phosphors are in a gel type leafy shape and $GaPO_4$: Sm^{3+} has shown, agglomerated spherical shape with average crystallite size, at around 100 nm. These phosphors have exhibited a strong reddish ($^4G_{5/2} \rightarrow {^6H_{9/2}}$) – orange ($^4G_{5/2} \rightarrow {^6H_{7/2}}$) color, upon UV- excitation. From the fluorescence spectra, it is obvious that the fluorescence behavior of these phosphors have strongly influenced with the concentration of gallium. On the basis of fluorescence and pertinent optical properties the phosphors with composition $Y_{0.95}PO_4$:$Sm_{0.05}^{3+}$ has suggested to be an appropriate luminescent material for their suitability in certain optical displays for reddish-orange color.

References

[1] K. Lai, B. Amurisana, Y. Yang, W. Xu, Y. Tao, H. Yang, J. Lumin. **128**, 52 (2008).

[2] J. Fu, Q. Zhang, Y. Li, H. Wang, J. Lumin. **130**, 231 (2010).

[3] J. Liao, S. Zhang, H. You, H. Wen, J. L. Chen, W. You, Opt. Mater. **33**, 953 (2011).

[4] X. Y. Chen, S. Bao, Y. Wu, J. Solid State Chem. **183**, 2004 (2010).

[5] X. Dou, W. Zhao, E. Song, G. Zhou, C. Yi, M. Zhou, Spectrochim. Acta A **78**, 821(2011).

[6] Z. H. Ju, R. P. Wei, J. X. Ma, C. R. Pang, W. S. Liu, J. Alloys Compd. **507**, 133 (2010).

[7] X. Li, L. Guan, X. Li, J. Wen, Z. Yang, Powder Tech. **200**, 12 (2010).

[8] Z. C. Wu, J. X. Shi, J. Wang, M. L. Gong, Q. Su, J. Solid State Chem. **179**, 2356 (2006).

[9] Y. Jin, W. P. Qin, J. S. Zhang, Y. Wang, C. Y. Cao, J. S. Zhang, X. G. Ren, G. F. Wang, G. D. Wei, L. L. Wang, L. J. Jin, L. P. F. Zhu, Mater. Lett. **62**, 3146 (2008).

[10] D. K. Yim, I. S. Cho, C. W. Lee, J. H. Noh, H. S. Roh, K. S. Hong, Opt. Mater. **33**, 1036 (2011).

[11] X. Zhang, H. J. Seo, J. Alloys Compd. **509**, 2007 (2011).

[12] J. S. Bae, B. K. Moon, B. C. Choi, J. H. Jeong, S. S. Yi, I. W. Kim, J. S. Lee, Thin Solid Films **424**, 291 (2003).

[13] J. H. Jeong, B. K. Moon, H. J. Seo, J. S. Bae, S. S. Yi, I. W. Kim, H. L. Park, Appl. Phys. Lett. **83**(7), 1346 (2003).

[14] T. Minami, T. Miyata, Y. Suzuki, Jpn. J. Appl. Phys. **14**, L684 (1995).

[15] M. Kizilyalli, A. J. E. Welch, J. Appl. Crystallogr, **9**, 413 (1976).

[16] R. Wang, W. Pan, J. Chen, M. Fang, Z. Cao, Y. Luo, Mater. Chem. Phys. **79**, 30 (2003).

[17] U. Rambabu, D. P. Amalnerkar, B. B. Kale, S. Buddhudu, Mater. Chem. Phys. **70**, 1 (2001).

[18] U. Rambabu, N. R. M. Rathnam, T. L. Prakash, S. Buddhudu, Mater. Chem. Phys. **78**, 160 (2002).

[19] M. K. Chong, K. Pita, C. H. Kam, J. Phys. Chem. Solids **66**, 213 (2005).

[20] B. K. Grandhe, V. R. Bandi, K. Jang, S. S. Kim, D. S. S. Shin, Y. I. Lee, J. M. Lim, T. Song, J. Alloys Compd. **509 (30)**, 7937 (2011).

[21] J. A. Diaz-Guillen, A. F. Fuentes, S. Gallini, M. T. Colomer, J. Alloys Compd. **427**, 87 (2007).

[22] S. Hachani, B. Moine, A. El-akrmi, M. Ferid, Opt. Mater. **31**, 678 (2009).

[23] D. Tu, Y. Liang, R. Liu, Z. Cheng, F. Yang, W. Yang, J. Alloys Compd. **509**, 5596 (2011).

[24] X. He, J. Zhou, N. Lian, J. Sun, M. Guan, J. Lumin. **130**, 743 (2010).

[25] L. Changmin, Y. Dianlai, Z. Yingying, W. Zhiqiang, L. Hai, J. Rare Earths **25**, 143 (2007).

[26] B. Lei, Y. Liu, G. Tang, Z. Ye, C. Shi, Mater. Chem. Phys. **87**, 227 (2004).

[27] V. Singh, S. Watanabe, T. K. Gundu Rao, J. F. D. Chubaci, H. Y. Kwak, J. Non- Cryst. Solids **356**, 1185 (2010).

[28] X. Liu, K. Han, M. Gu, L. Xiao, C. Ni, S. Huang, B. Liu, Solid State Commun. **142**, 680 (2007).

[29] X. Yu, X. Xu, C. Zhou, J. F. Tang, X. D. Peng, S. Yang, Mater. Res. Bull. **41**, 1578 (2006).

_____

*Corresponding author: sdhan@kier.re.kr